



## MHD CASSON OR CARREAU FLUIDS FLOW WITH MICROORGANISMS OVER A PERMEABLE SHRINKING SURFACE

Nepal Chandra Roy<sup>1</sup>, Goutam Saha<sup>1,\*</sup>, Suvash C. Saha<sup>2</sup>

<sup>1</sup>Department of Mathematics, University of Dhaka, Dhaka 1000, Bangladesh, Email address [Nepal@du.ac.bd](mailto:Nepal@du.ac.bd)

<sup>2</sup>School of Mechanical & Mechatronics Engineering, University of Technology Sydney (UTS), NSW 2007, Australia, Email address [Suvash.Saha@uts.edu.au](mailto:Suvash.Saha@uts.edu.au)

\*Corresponding Author's Email address: [gsahamath@du.ac.bd](mailto:gsahamath@du.ac.bd)

### Abstract:

The characteristics of dual solutions of the flow of Casson or Carreau fluids mixed with microorganisms over a permeable shrinking surface are investigated considering the effects of the magnetic field, heat dissipation, Dufour, and thermophoretic diffusivity. By using similarity transformations, the governing equations are converted into a set of ordinary differential equations. These reduced equations are then solved by the well-known shooting technique along with the fourth-order Runge-Kutta method. A comparison is provided and the present solutions hold a good agreement with available published results. The local skin friction coefficient, local Nusselt number, local Sherwood number, and local density number of the microorganisms are found to increase with the increase of non-Newtonian Casson parameter, Dufour, and thermophoretic diffusivity number, however, it decreases with Weissenberg number. The remarkable finding which is not revealed yet is that dual solutions exist in the flow of Casson or Carreau fluids with microorganisms over a permeable shrinking sheet subject to a certain combination of parameters. Moreover, the domain of the occurrence of dual solutions broadens on account of higher values of all physical parameters of the problem except the Eckert number.

**Keywords:** Microorganisms; Casson fluid; Carreau fluid; Magnetohydrodynamic; Permeable surface.

### NOMENCLATURE

$B_0$	Magnetic field strength	$T$	Fluid's temperature
$C$	Fluid's concentration	$T_w$	Wall temperature
$C_s$	Concentration susceptibility	$C_w$	Wall Concentration
$C_p$	Heat capacities of the fluid	$M_w$	Wall density of microorganisms
$D_B$	Brownian diffusion	$T_\infty$	Temperature outside the boundary layer
$D_n$	Microorganisms diffusion	$C_\infty$	Concentration outside the boundary layer
$D_T$	Thermal diffusion	$M_\infty$	Density outside the boundary layer
$D_f$	Dufour number	$u, v$	Velocities in $x$ and $y$ directions
$Ec$	Eckert number	$We$	Weissenberg number
$g$	Acceleration due to the gravity	<b>Greek symbols</b>	
$Gr_T$	Momentum buoyancy parameter	$\sigma$	Magnetic field strength
$Gr_C$	Concentration buoyancy parameter	$\nu$ & $\nu_c$	Viscosity of the fluid and microorganisms
$Ha$	Hartman Number	$\delta$	Boundary layer thickness
$\bar{K}$	Thermal diffusion ratio	$\rho$	Density of the fluid
$\bar{K}$	Permeability constant	$\kappa'$	Permeability constant
$M$	Microorganisms mass density	$b$	Constant
$N_b$	Brownian diffusivity number	$\beta$	Shrinking parameter
$N_t$	Thermophoretic diffusivity number	$\Gamma$	Variable time

$Nn$	Density number of the microorganisms	$l$	Characteristic length
$Nu$	Nusselt number	$\Phi$	Heat dissipation
$Pe$	Peclet number	$\kappa$	Thermal conductivity
$Pr$	Prandtl number	$\beta_T$	Volumetric coefficients due to thermal
$Sb$	Schmidt number for microorganisms	$\beta_C$	Volumetric coefficients due to C
$Sc$	Schmidt number	$\beta_M$	Microorganisms coefficient due to M
$Sh$	Sherwood number	$\sigma_1$	Mass concentration parameter

## 1. Introduction

Flow over a horizontal or vertical plate, stretching or shrinking sheet, porous surface, with or without the presence of magnetic/electric field are of interest of many researchers over the years. Also, many researchers carried out a theoretical or numerical study to find the dual solution of the above mentioned problem. Ishak et al. (2008) studied numerically the mixed convection flow on a permeable vertical plate and observed the dual solution of the problem. Later, Ishak et al. (2009) carried out a similar study for micropolar fluids. In these study, they first transformed the set of nonlinear PDE into nonlinear ODE and then used the finite difference method to formulate and solve the problem. Their results reveal that dual solutions can be observed for the assisting flow. Also, Xu and Liao (2008) studied the flow over a flat plate and obtained the dual solution using the Homotopy analysis method. Their results are compared with numerical solutions and found a good agreement. It suggests that this method can be very useful for solving nonlinear system. Moreover, Subhashini et al. (2012) numerically investigated the dual solution behavior of flow over a porous flat plate with suction or injection. They used the nonlinear shooting method with the Runge-Kutta method of 4th order to solve the converted non-linear ODE. It is observed that the dual solutions of velocity, temperature and concentration profiles can be found for some particular parameters. Later, Subhashini and Sumathi (2014) used numerical approach to find the dual solution of nanofluids flow over moving vertical plate. They used a numerical approach discussed in Subhashini et al. (2012). They considered three different types of nanofluids and found that the existence of dual solution is possible. Some of the similar research is mentioned in Khashiie et al. (2021).

Turkyilmazoglu (2012) studied theoretically the dual and triple solutions behavior of electrically conducting non-Newtonian MHD fluid flow past a shrinking sheet. It is seen that multiple solution exists for some small group of parameters. Moreover, Zheng et al. (2012) carried out a theoretical investigation to observe the dual solution for micropolar fluid flow over stretching/shrinking sheet. They also used Homotopy analysis method for theoretical framework of the problem. Bhattacharyya (2011) numerically studied the mass transfer behavior in the presence of chemical reaction of flow over stretching or shirking sheet. He also transformed the nonlinear system of PDE into a nonlinear system of ODE using similarity transformations and then solved the system by the well-known nonlinear shooting method. It is found that the dual solutions of velocity and concentration can be observed for some parameters. Singh and Chamkha (2013) investigated numerically the dual solution of flow over vertical porous shrinking sheet. Subhashini et al. (2013) carried out a numerical study of the dual solutions of non-Newtonian fluid flow over stretching sheet with variable thickness. Akbar et al. (2014) carried out numerical procedure to find the dual solution of MHD Carreau fluid flow over the porous shrinking sheet. Singh and Chamkha (2013), Subhashini et al. (2013) and Akbar et al. (2014) used the same numerical approach proposed by Subhashini et al. (2012). Sandeep and Sulochana (2015) studied unsteady micropolar fluid flow over stretching/shrinking sheet with non-uniform heat source/sink. They used the nonlinear shooting method with the available packages in Matlab. All the above mentioned authors observed that dual solution is feasible. El-Aziz (2016) carried out a research on MHD incompressible fluid flow over stretching/shrinking sheet with non-uniform heat source/sink. He used the nonlinear shooting method with Runge-Kutta-Fehlberg fifth order scheme. He showed the dual solutions for different parameters and presented them graphically in terms of velocity and temperature. Recently, Lund et al. (2019) studied the Williamson fluid flow over an exponentially vertical shrinking sheet with variable thickness and thermal conductivity. They used Runge-Kutta shooting method and used maples for simulations. They also found dual solutions for different parameters. In addition, some of the relevant research works have been cited in (Ghosh et al., 2016; Freidoonimehr & Rahimi, 2017; Khan et al., 2017; Hamid et al., 2019; Haq et al., 2020; Roy, 2020; Mousavi et al., 2021; Asogwa & Ibe, 2020; Nagendra et al., 2022; Roy & Saha, 2022).

From the above literature reviews, it is seen that very little attention has been given by the researcher on the investigation of the dual solutions of Casson or Carreau fluid flow over a porous surface. However, in recent years, presence of microorganism in the fluids creates a huge interest in the CFD research community (Atif et al., 2019; Mondal & Pal, 2020; Yusuf et al., 2021; Biswas et al., 2021). With authors' knowledge, the use of both Casson and Carreau fluids in a same model were presented by Raju and Sandeep (2016). Later, Mahanthesh et al. (2019) used this idea for dusty Casson and Carreau fluids. These works influenced us to use both non-Newtonian fluids (Casson or Carreau fluids) in a same model. Open literature suggests that no research has taken an attempt to investigate the dual solutions for the flow of Casson and Carreau fluids with microorganisms over a shrinking sheet. So, the objective of this study is to examine the dual solutions of the flow of MHD Casson and Carreau fluids combined with microorganisms over permeable stretching sheet. The governing equations are reduced to a set of nonlinear differential equations using similarity transformations. We solve the resulting equation using the nonlinear shooting method. Results are discussed in terms of dual solutions for varying relevant parameters.

## 2. Mathematical Model

We consider two dimensional steady MHD Casson or Carreau fluids flow with microorganisms over a permeable shrinking surface. The flow configuration with boundary conditions are elucidated in Fig. 1. Here  $x$  and  $y$  measure the distances along and normal to the shrinking sheet. Also,  $u$  and  $v$  are the velocity components in the  $x$ - and  $y$ -direction,  $u_w(x)$  is the shrinking velocity of the plate,  $v_w$  is the mass flux through the plate,  $T_w, C_w, M_w$  are the wall temperature, concentration, density of microorganisms and  $T_\infty, C_\infty, M_\infty$  are the corresponding quantities outside the boundary layer. In the figure,  $\delta_u, \delta_T, \delta_C, \delta_M$  are respectively the boundary layer thicknesses for momentum, thermal, concentration and microorganisms. Definition of tensor for Casson and Carreau fluids is presented in Raju and Sandeep (2016) and used in this study.

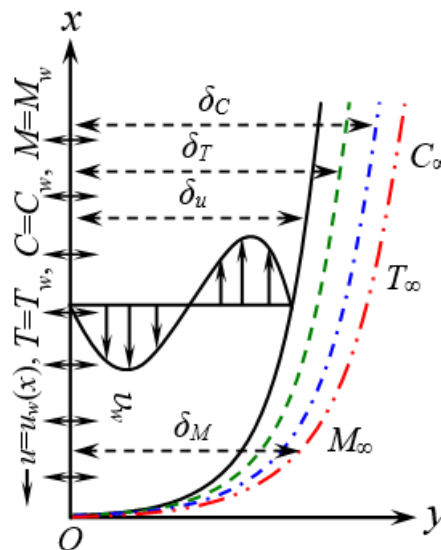


Fig. 1: Physical model with boundary conditions

Moreover, the thermophysical properties of the fluid are taken to be constant. Under the usual Boussinesq approximation, the governing equations for Casson or Carreau fluids flow with microorganisms are, following (Raju & Sandeep, 2016; Mahanthesh et al., 2019; Qasim & Noreen, 2014; Saravana et al., 2019; Waqas et al., 2021):

$$\frac{\partial u}{\partial x} + \frac{\partial v}{\partial y} = 0, \tag{1}$$

$$u \frac{\partial u}{\partial x} + v \frac{\partial u}{\partial y} = \nu \left( 1 + \frac{1}{\beta} \right) \frac{\partial^2 u}{\partial y^2} + \frac{3}{2} \nu (n-1) \Gamma^2 \left( \frac{\partial u}{\partial y} \right)^2 \frac{\partial^2 u}{\partial y^2} - \left( \frac{\sigma B_0^2}{\rho} + \frac{\nu}{\kappa'} \right) u + g\beta_T(T - T_\infty) + g\beta_C(C - C_\infty), \tag{2}$$

$$u \frac{\partial T}{\partial x} + v \frac{\partial T}{\partial y} = \frac{\nu}{C_p} \left(1 + \frac{1}{\beta}\right) \left(\frac{\partial u}{\partial y}\right)^2 + \frac{\kappa}{\rho C_p} \frac{\partial^2 T}{\partial y^2} + \frac{D_m \bar{\kappa}}{C_s C_p} \frac{\partial^2 C}{\partial y^2}, \tag{3}$$

$$u \frac{\partial C}{\partial x} + v \frac{\partial C}{\partial y} = D_B \frac{\partial^2 C}{\partial y^2} + \frac{D_T}{T_\infty} \frac{\partial^2 T}{\partial y^2}, \tag{4}$$

$$u \frac{\partial M}{\partial x} + v \frac{\partial M}{\partial y} + \frac{b\nu_c}{C_w - C_\infty} \frac{\partial}{\partial y} \left(M \frac{\partial C}{\partial y}\right) = D_n \frac{\partial^2 M}{\partial y^2}, \tag{5}$$

with boundary conditions

$$u = u_w(x) = -bx, v = v_w \text{ at } y = 0, \tag{6}$$

$$u \rightarrow 0 \text{ as } y \rightarrow \infty, \tag{7}$$

$$T = T_w, C = C_w, M = M_w \text{ at } y = 0, \tag{8}$$

$$T \rightarrow T_\infty, C \rightarrow C_\infty, M \rightarrow M_\infty \text{ as } y \rightarrow \infty. \tag{9}$$

In the above equations,  $\beta$  is the non-Newtonian Casson parameter,  $n$  is the power-law index,  $\sigma$  is the magnetic field strength,  $\nu$  and  $\nu_c$  are the viscosity of the fluid and microorganisms,  $D_m$  is the chemical molecular diffusivity,  $D_B$ ,  $D_n$  and  $D_T$  are material, Brownian, microorganisms and thermal diffusions,  $C_s$  is the concentration susceptibility, and  $C_p$  are the heat capacities of the material and fluid,  $\rho$  is the density of the fluid,  $\kappa'$  is the permeability constant,  $B_0$  is the strength of the magnetic field considered normal to the sheet,  $C$  is the concentration of the fluid,  $M$  is the mass density of the microorganisms,  $g$  is the acceleration due to the gravity,  $\Gamma$  is the time constant,  $\kappa$  is the thermal conductivity,  $\bar{\kappa}$  is the thermal diffusion ratio,  $\beta_T$  and  $\beta_C$  are the volumetric coefficients due to thermal and concentration expansions. In this study, we also assume that  $\beta \rightarrow \infty$  for Carreau fluid and  $\Gamma = 0$  for Casson fluid.

Let us introduce the following transformations:

$$u = bx f'(\eta), v = -\sqrt{b\nu} f(\eta), \eta = \sqrt{\frac{b}{\nu}} y$$

$$\theta(\eta) = \frac{T - T_\infty}{T_w - T_\infty}, \varphi(\eta) = \frac{C - C_\infty}{C_w - C_\infty}, \chi(\eta) = \frac{M - M_\infty}{M_w - M_\infty}, \tag{10}$$

Applying the transformations given in Eq. (10) in the Eqs. (1)-(9), the following non-dimensional non-linear ordinary differential equations and corresponding boundary conditions are obtained:

Non-dimensional governing equations:

$$\left(1 + \frac{1}{\beta}\right) f''' + \frac{3}{2} (n - 1) We^2 f''' (f'')^2 + f f'' - (f')^2 - (Ha^2 + \bar{K}) f' + Gr_T \theta + Gr_C \varphi = 0, \tag{11}$$

$$\frac{1}{Pr} \theta'' + f \theta' + Ec \left(1 + \frac{1}{\beta}\right) (f'')^2 + D_f \varphi'' = 0, \tag{12}$$

$$\frac{1}{S_c} \varphi'' + f \varphi' + \frac{1}{S_c} \frac{N_t}{N_b} \theta'' = 0, \tag{13}$$

$$\chi'' + S_b \chi' f - Pe[(\sigma_1 + \chi)\varphi'' + \chi' \varphi'] = 0, \tag{14}$$

where,

$$Ha^2 = \frac{\sigma B_0^2}{b\rho}, \bar{K} = \frac{\nu}{b\kappa'}, Gr_T = \frac{g\beta_T(T_w - T_\infty)}{b\nu_w}, Gr_C = \frac{g\beta_C(C_w - C_\infty)}{b\nu_w}, Pr = \frac{\nu}{\alpha}, \alpha = \frac{\kappa}{\rho C_p},$$

$$Ec = \frac{u_w^2}{C_p(T_w - T_\infty)}, D_f = \frac{D_m \bar{\kappa} (C_w - C_\infty)}{C_s C_p \nu (T_w - T_\infty)}, N_b = \frac{\tau D_B (C_w - C_\infty)}{\nu}, N_t = \frac{\tau D_T (T_w - T_\infty)}{\nu T_\infty},$$

$$S_c = \frac{\nu}{D_B}, We^2 = \frac{b u_w^2}{\nu} \Gamma^2, Pe = \frac{b \nu_c}{D_n}, S_b = \frac{\nu}{D_n}, \sigma_1 = \frac{M_\infty}{M_w - M_\infty}.$$

Here  $Ha$  is the Hartman number,  $\bar{K}$  is the permeability constant,  $Gr_T$  is the Grashof number for thermal diffusion,  $Gr_C$  is the Grashof number for mass diffusion,  $Pr$  is the Prandtl number,  $Ec$  is the Eckert number,  $D_f$  is the Dufour number,  $N_b$  is the Brownian diffusivity number,  $N_t$  is the thermophoretic diffusivity parameter,  $We$  is the Weissenberg number,  $Pe$  is the Peclet number,  $S_c$  is Schmidt number,  $S_b$  is Schmidt number for microorganisms diffusivity and  $\sigma_1$  is the mass concentration parameter.

Non-dimensional boundary conditions are

$$f(\eta) = S, f'(\eta) = -1 \text{ at } \eta = 0, \tag{15}$$

$$f'(\eta) \rightarrow 0 \text{ as } \eta \rightarrow \infty, \tag{16}$$

$$\theta(\eta) = 1, \varphi(\eta) = 1, \chi(\eta) = 1 \text{ at } \eta = 0, \tag{17}$$

$$\theta(\eta) \rightarrow 0, \varphi(\eta) \rightarrow 0, \chi(\eta) \rightarrow 0 \text{ as } \eta \rightarrow \infty. \tag{18}$$

where,  $S = -\frac{v_w}{\sqrt{vb}}$  is the suction or injection parameter.

In this study, the local skin friction coefficient (Hayat et al., 2012), the local Nusselt number (Hayat et al., 2012; Waqas et al., 2021), the local Sherwood number (Hayat et al., 2012; Waqas et al., 2021), and the local density number of the microorganisms (Waqas et al., 2021) are defined by

$$\left. \begin{aligned} Re_x^{1/2} C_f &= \left(1 + \frac{1}{\beta}\right) f''(0), \\ Re_x^{-1/2} Nu_x &= -\theta'(0), \\ Re_x^{-1/2} Sh_x &= -\varphi'(0), \\ Re_x^{-1/2} Nn_x &= -\chi'(0), \end{aligned} \right\} \tag{19}$$

where,  $Re_x$  is the local Reynolds number.

### 3. Numerical Methods and Validations

The system of equations (11)-(14) along with the boundary conditions (15)-(18) are solved by the non-linear shooting method combined with Runge-Kutta technique of order four. The flow chart of the method is shown in Fig. 2. To convert the Eqs. (11)-(14) into first order ODEs, let us introduce the following transformations:

$$f = y_1, f' = y_2, f'' = y_3, \theta = y_4, \theta' = y_5, \varphi = y_6, \varphi' = y_7, \chi = y_8, \chi' = y_9. \tag{20}$$

Using the above transformations, we get the following system of ODEs:

$$\left. \begin{aligned} y_1' &= y_2, \\ y_2' &= y_3, \\ y_3' &= \frac{y_2^2 - y_1 y_3 - (Ha^2 + \bar{K})y_2 - Gr_T y_4 - Gr_C y_6}{\left(1 + \frac{1}{\beta}\right) + \frac{3}{2}(n-1)We^2 y_3^2}, \\ y_4' &= y_5, \\ y_5' &= -Pr \left\{ y_1 y_5 + Ec \left(1 + \frac{1}{\beta}\right) y_3^2 + D_f y_7' \right\}, \\ y_6' &= y_7, \\ y_7' &= -Sc \left( y_1 y_7 + \frac{1}{Sc} \frac{N_t}{N_b} y_5' \right), \\ y_8' &= y_9, \\ y_9' &= Pe \{ (\sigma_1 + y_8) y_7' + y_7 y_9 \} - Sb y_1 y_9, \end{aligned} \right\} \tag{21}$$

And the corresponding boundary conditions are

$$\left. \begin{aligned} y_1 = S, y_2 = -1, y_4 = 1, y_6 = 1, y_8 = 1 \text{ at } \eta = 0 \\ y_2 \rightarrow 0, y_4 \rightarrow 0, y_6 \rightarrow 0, y_8 \rightarrow 0 \text{ as } \eta \rightarrow \infty \end{aligned} \right\} \tag{22}$$

In order to solve the above transformed system using the nonlinear shooting method, we need to guess four initial conditions, such as  $y_3(0) = p_1, y_5(0) = p_2, y_7(0) = p_3, y_9(0) = p_4$ . The four unknowns  $p_1, p_2, p_3, p_4$  are chosen in such a way that these four boundary conditions are satisfied for  $\eta \rightarrow \infty$ . The numerical simulations are performed for suitable domain  $[0, \eta_{max}]$  in place of the domain  $[0, \infty)$  where we choose  $\eta_{max} \in \mathbb{R}^+$  very carefully so that higher values of  $\eta_{max}$  showed insignificant variation for all the outcomes. Moreover, convergence criteria are set as the following:

$$\max\{y_i - 0\} < 10^{-6}, i = 1,2,4,6,8 \tag{23}$$

Validation is carried out by comparing the first and second solutions of  $-\theta'(0)$  with the results of Qasim and Noreen (2014) as shown in Table 1. An excellent agreement is observed which motivated us to move to the next step.

Table 1: Comparison of  $-\theta'(0)$

$S$	$\beta$	Qasim and Noreen (2014)		Present Method	
		First solution	Second solution	First solution	Second solution
2.4	3.0	0.80814	0.88288	0.80814	0.88377
2.7	3.0	0.91197	1.13797	0.91201	1.13905
3.0	3.0	1.01955	1.39641	1.01957	1.40754
2.5	2.0	0.86406	0.93142	0.86401	0.93123
2.5	10.0	0.82813	0.99868	0.82815	0.99756

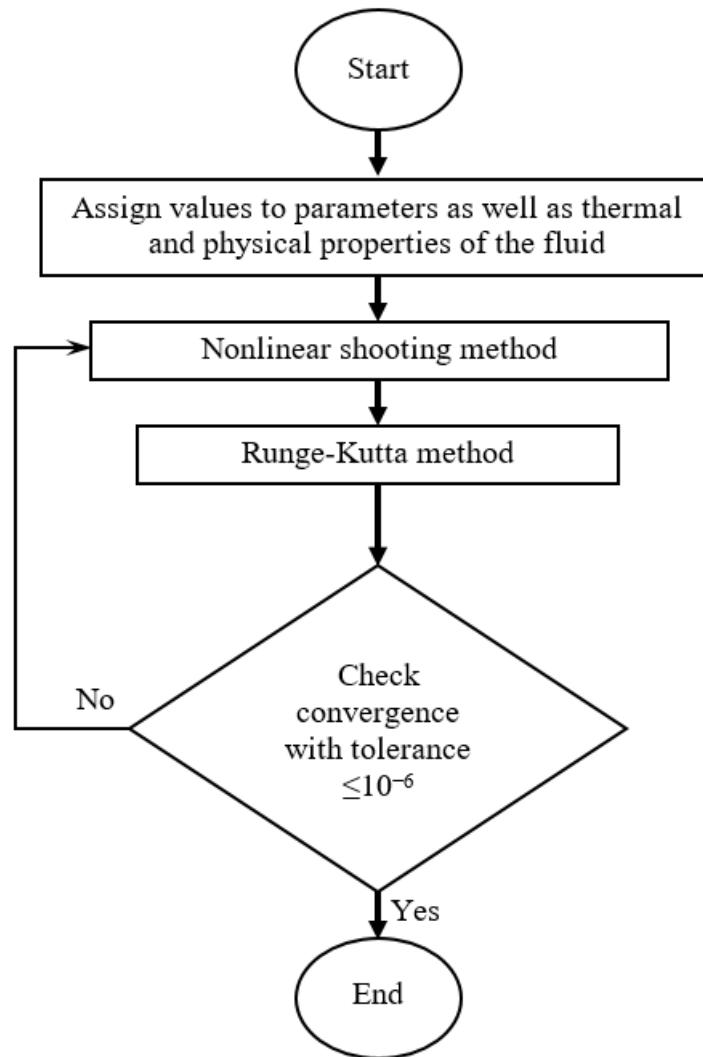


Fig. 2: Flow chart of the solution scheme

#### 4. Results and Discussion

In this investigation, the values of the parameters are collected from the open literatures. Here, we consider  $Pr = 0.71$ ,  $Ha = 0$  to  $0.6$ ,  $S = 1$  to  $6$  (Mousavi et al., 2021),  $\beta = 0.2$  to  $0.8$ ,  $We = 1$  to  $5$  (Raju & Sandeep, 2016) and  $Ec = 0$  to  $0.5$  (Ullah et al., 2019).

Influences of  $N_t$  on  $Re_x^{1/2} C_f$ ,  $Re_x^{-1/2} Nu_x$ ,  $Re_x^{-1/2} Sh_x$ , and  $Re_x^{-1/2} Nn_x$  are shown in Fig. 3 and Table 2. All of these important quantities decrease owing to the reduction in the suction parameter,  $S$ . With the increase of  $N_t$

the values of  $Re_x^{1/2}C_f$  and  $Re_x^{-1/2}Nu_x$  are found to increase whereas the values of  $Re_x^{-1/2}Sh_x$  and  $Re_x^{-1/2}Nn_x$  decrease. On the other hand, for a fixed set of parameter there exist dual solutions consisting of stable and unstable solutions. The upper branch represents stable solutions and the lower branch shows unstable solutions. It is noted that stable solutions are of physical interest and can be validated by experiment. As  $N_t$  increases, dual solutions exist in a wider domain of  $S$ . This indicates that when thermophoretic diffusivity is higher, boundary layer separation takes place for a smaller suction parameter. The parameter  $N_t$  is defined as the ratio of thermal diffusivity to viscous force. So, the value of  $N_t$  becomes higher for larger thermal diffusivity and lower viscous force. As a consequence, when  $N_t$  is higher the boundary layer separates from the sheet for smaller suction parameter.

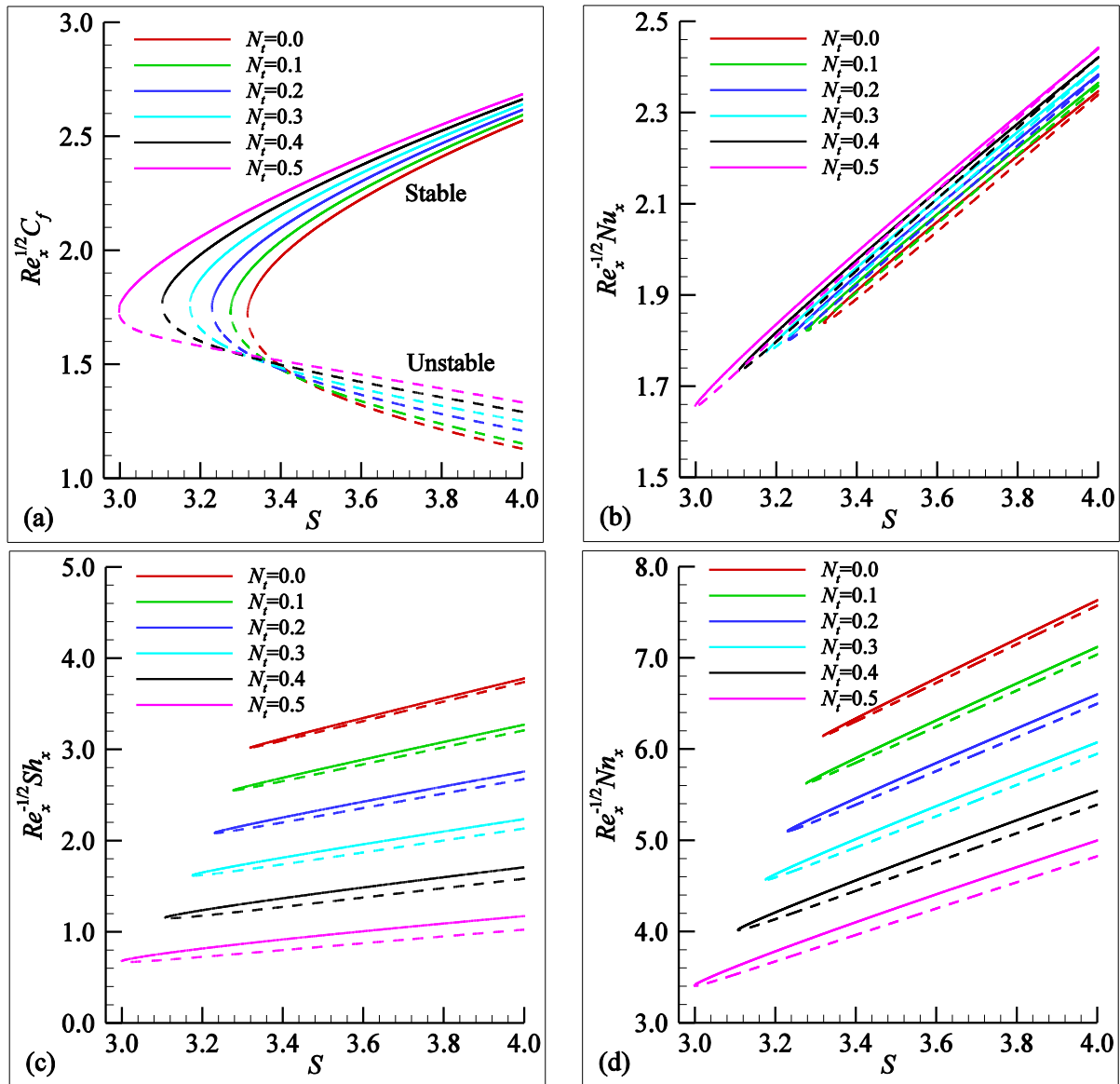


Fig. 3: Values of  $Re_x^{1/2}C_f$ ,  $Re_x^{-1/2}Nu_x$ ,  $Re_x^{-1/2}Sh_x$ , and  $Re_x^{-1/2}Nn_x$  when  $Pr=0.7$ ,  $Pe=1.0$ ,  $\beta=0.5$ ,  $Ha=0.1$ ,  $D_f=0.05$ ,  $Ec=0.1$ ,  $We=1.0$ .

Figure 4 and Table 2 depict the changes of  $Re_x^{1/2}C_f$ ,  $Re_x^{-1/2}Nu_x$ ,  $Re_x^{-1/2}Sh_x$ , and  $Re_x^{-1/2}Nn_x$  with non-Newtonian Casson parameter,  $\beta$ . It is clear from the figures that an increase in  $\beta$  enhances the values of  $Re_x^{-1/2}Nu_x$ ,  $Re_x^{-1/2}Sh_x$ , and  $Re_x^{-1/2}Nn_x$ , whereas they decrease with lower value of  $S$ . Contrary to this, when  $\beta$  is increased the skin friction coefficient decreases in a region for  $S \geq 3.5$  and it increases in a region for  $S$

$\leq 3.5$ . Moreover, the domain of dual solutions increases for higher  $\beta$ . As the increasing  $\beta$  reduces the viscous force and heat dissipation, hence it delays the boundary layer separation in terms of  $S$ .

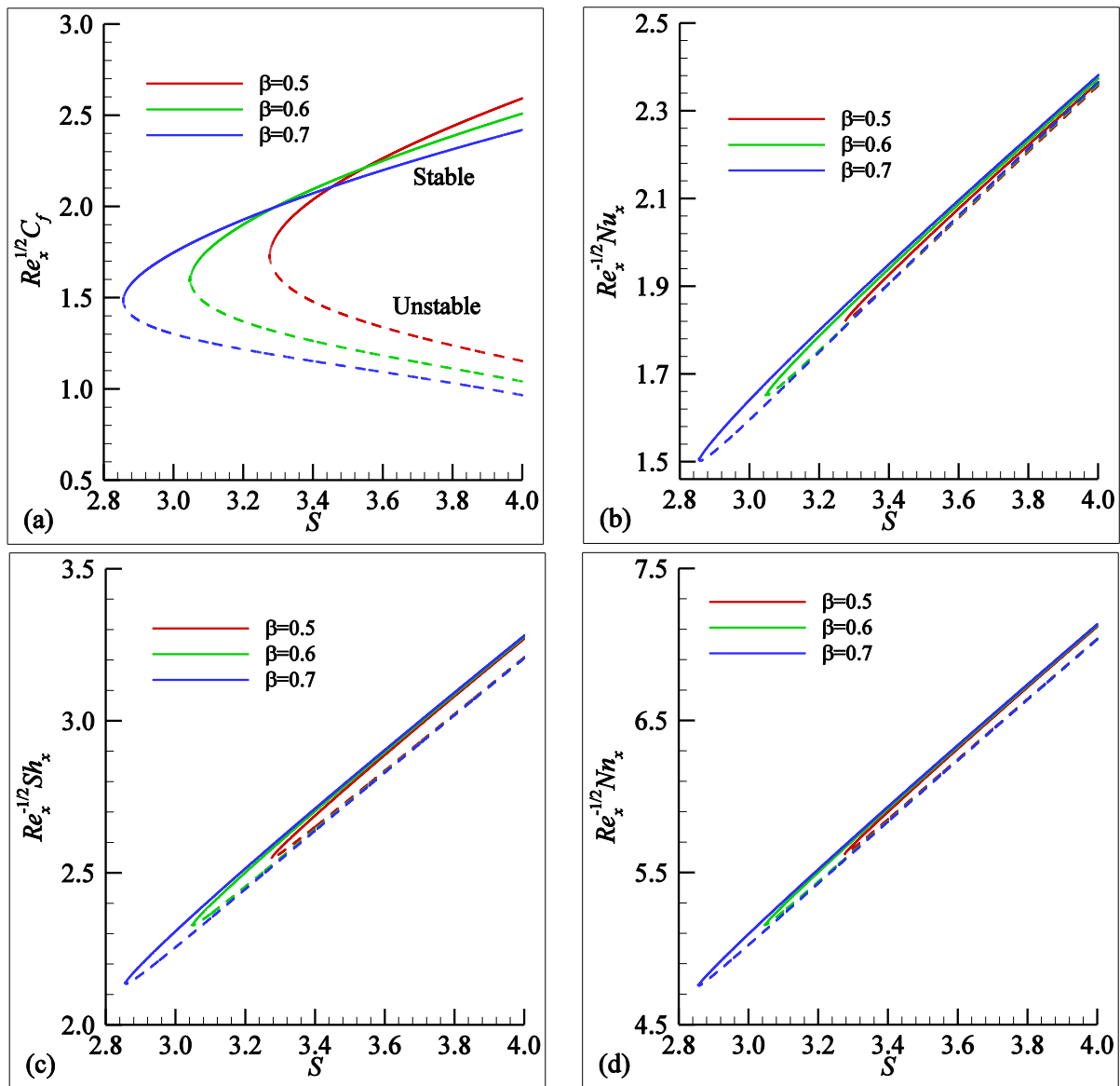


Fig. 4: Values of  $Re_x^{1/2} C_f$ ,  $Re_x^{-1/2} Nu_x$ ,  $Re_x^{-1/2} Sh_x$ , and  $Re_x^{-1/2} Nn_x$  when  $Pr=0.7$ ,  $Pe=1.0$ ,  $Ha=0.1$ ,  $Ni=0.1$ ,  $D_f=0.05$ ,  $Ec=0.1$ ,  $We=1.0$ .

The effects of the Dufour number,  $D_f$ , on  $Re_x^{1/2} C_f$ ,  $Re_x^{-1/2} Nu_x$ ,  $Re_x^{-1/2} Sh_x$ , and  $Re_x^{-1/2} Nn_x$  are elucidated in Fig. 5 and Table 2. As  $D_f$  increases, values of  $Re_x^{1/2} C_f$ ,  $Re_x^{-1/2} Sh_x$ , and  $Re_x^{-1/2} Nn_x$  significantly increase, however,  $Re_x^{-1/2} Nu_x$  drastically decreases. Additionally, increasing  $D_f$  augments the domain of the existence of dual solutions. For any value of  $D_f$  all of the important physical quantities diminish by increasing  $S$ . From the definition,  $D_f$  measures the relative mass diffusion with the change of enthalpy. As a result, Dufour number,  $D_f$ , increases for higher mass diffusion with smaller enthalpy change. Such a phenomena augments  $Re_x^{1/2} C_f$ ,  $Re_x^{-1/2} Sh_x$ , and  $Re_x^{-1/2} Nn_x$  but it diminishes  $Re_x^{-1/2} Nu_x$ . In addition, for higher  $D_f$  the boundary layer separation takes place with smaller  $S$ .



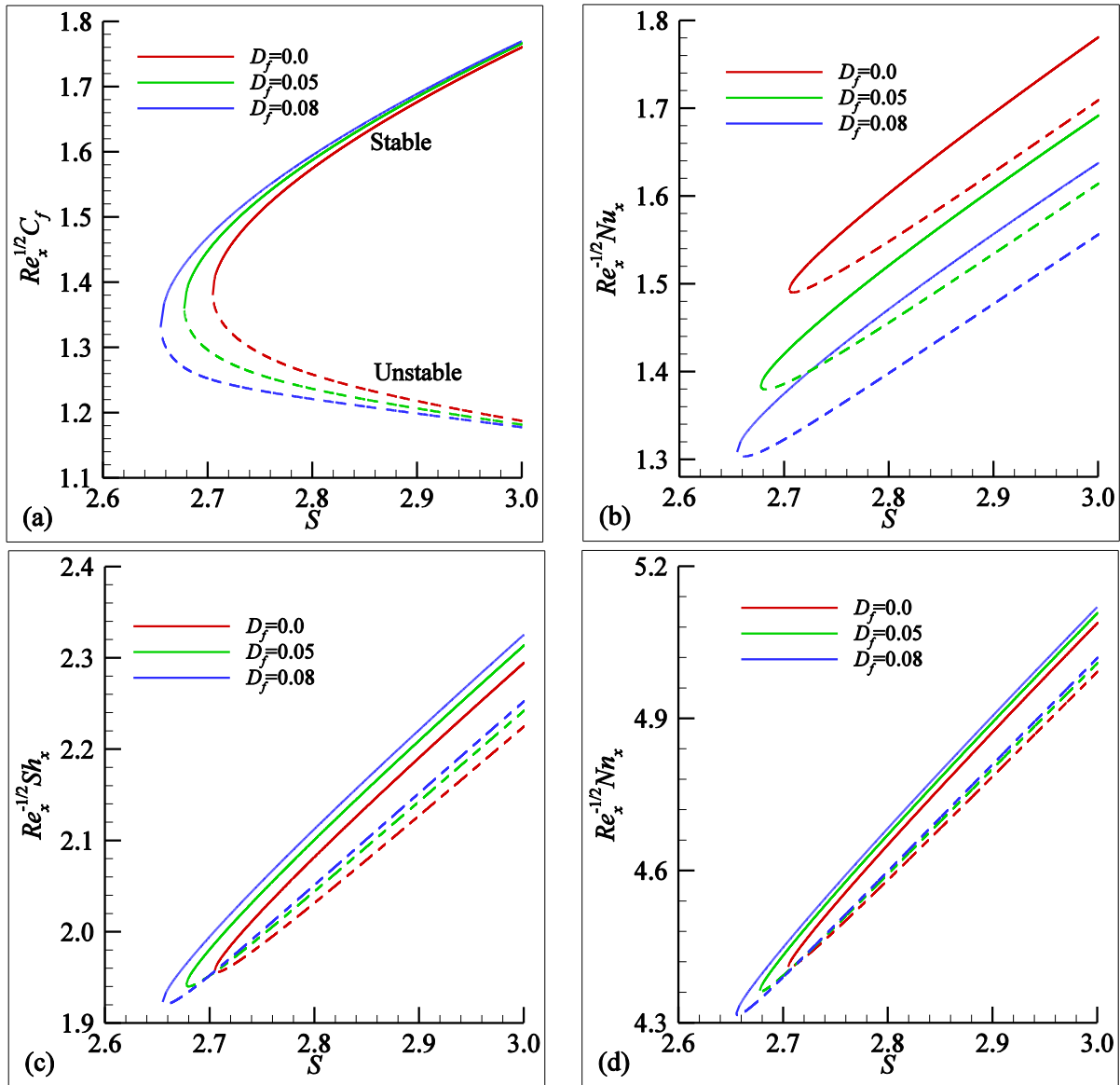


Fig. 5: Values of  $Re_x^{1/2} C_f$ ,  $Re_x^{-1/2} Nu_x$ ,  $Re_x^{-1/2} Sh_x$ , and  $Re_x^{-1/2} Nn_x$  when  $Pr=0.7$ ,  $Pe=1.0$ ,  $\beta=0.8$ ,  $Ha=0.1$ ,  $N_f=0.1$ ,  $Ec=0.1$ ,  $We=1.0$ .

In Fig. 6 and Table 2, the influences of the Eckert number on  $Re_x^{1/2} C_f$ ,  $Re_x^{-1/2} Nu_x$ ,  $Re_x^{-1/2} Sh_x$ , and  $Re_x^{-1/2} Nn_x$  are presented. Results revealed that increases, higher  $Ec$  leads to an increase in  $Re_x^{1/2} C_f$ ,  $Re_x^{-1/2} Sh_x$ , and  $Re_x^{-1/2} Nn_x$ , but it diminishes the value of  $Re_x^{-1/2} Nu_x$ . When  $S$  is increased, the above quantities are found to decrease. Also, dual solutions exist over a larger domain with the increase of  $Ec$ . It is evident from the definition of  $Ec$  that when  $Ec$  is higher the kinetic energy is higher with respect to smaller enthalpy difference. That is why, larger  $Ec$  gives rise to a significant increase in  $Re_x^{1/2} C_f$ ,  $Re_x^{-1/2} Sh_x$ , and  $Re_x^{-1/2} Nn_x$ , whereas a decrease in  $Re_x^{-1/2} Nu_x$ .

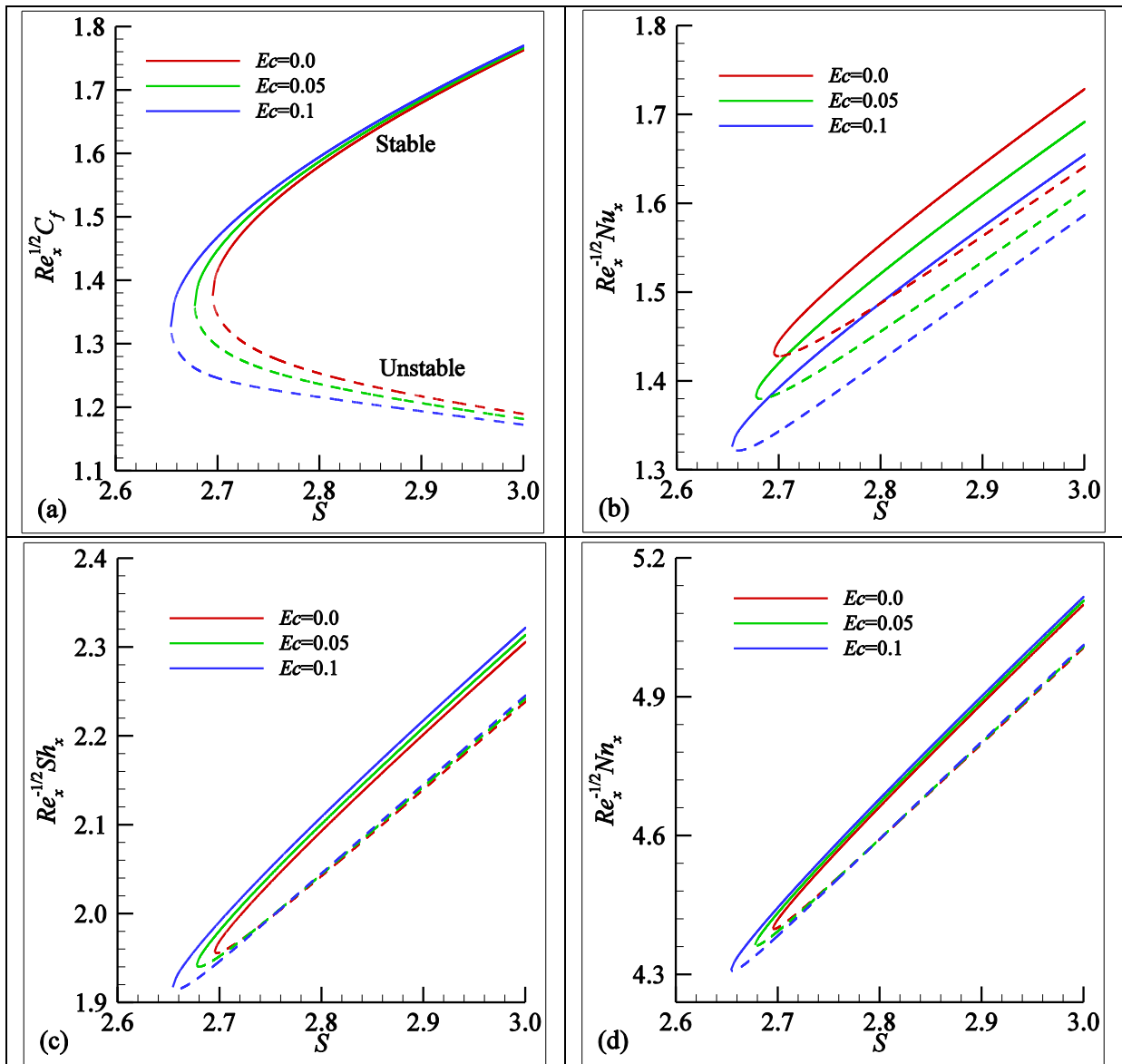


Fig. 6: Values of  $Re_x^{1/2} C_f$ ,  $Re_x^{-1/2} Nu_x$ ,  $Re_x^{-1/2} Sh_x$ , and  $Re_x^{-1/2} Nn_x$  when  $Pr=0.7$ ,  $Pe=1.0$ ,  $\beta=0.8$ ,  $Ha=0.1$ ,  $N_f=0.1$ ,  $D_f=0.05$ ,  $We=1.0$ .

Fig. 7 and Table 2 demonstrate the effects of  $We$  on  $Re_x^{1/2} C_f$ ,  $Re_x^{-1/2} Nu_x$ ,  $Re_x^{-1/2} Sh_x$ , and  $Re_x^{-1/2} Nn_x$ . It is evident from the results that all of the quantities are found to decrease for higher  $We$  and decreasing of  $S$ . Moreover, the domain of dual solutions reduces with increasing  $We$ . This is due to the fact that the higher shearing rate retards the flow and energy transfer.

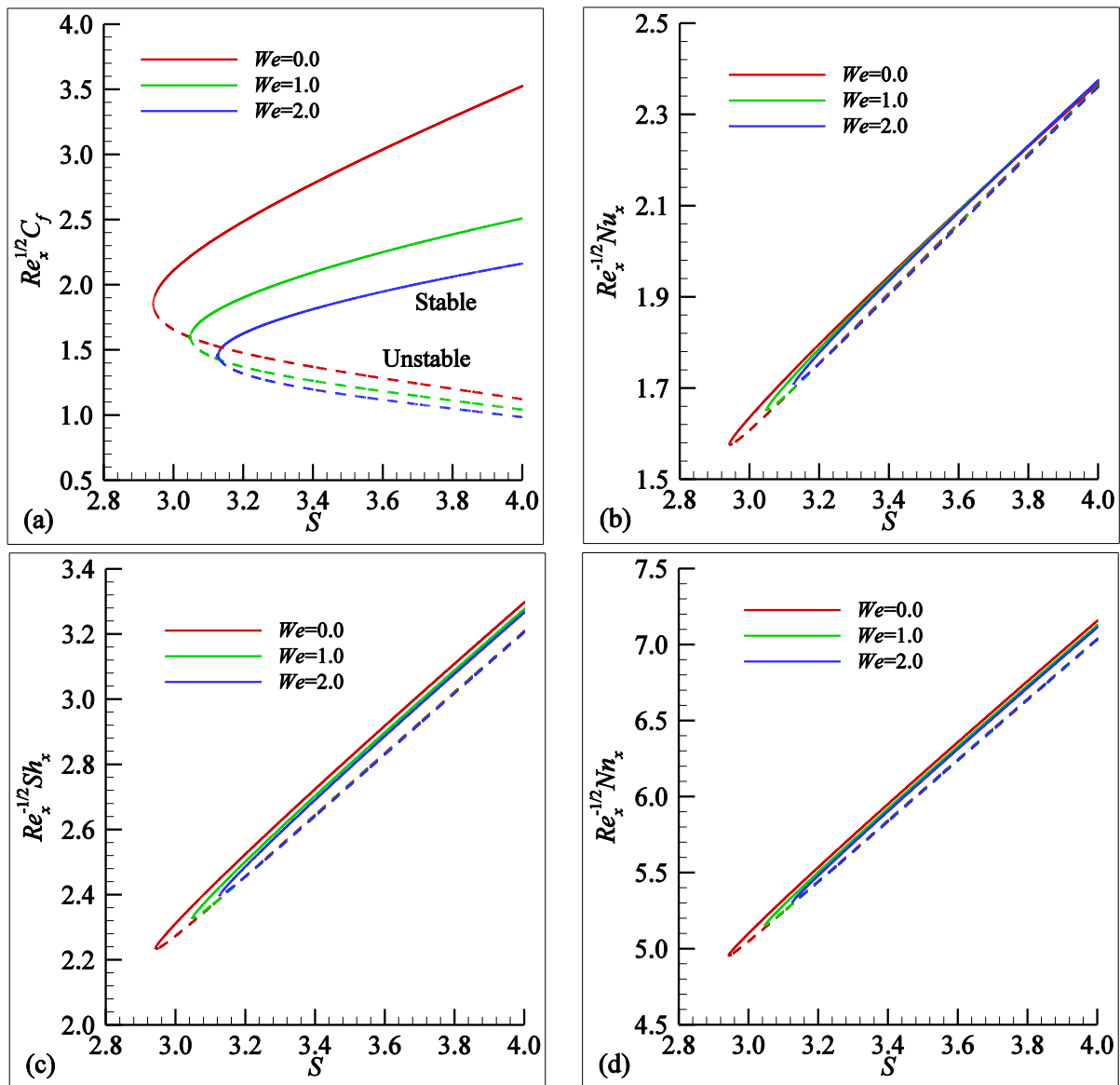


Fig. 7: Values of  $Re_x^{1/2} C_f$ ,  $Re_x^{-1/2} Nu_x$ ,  $Re_x^{-1/2} Sh_x$ , and  $Re_x^{-1/2} Nn_x$  when  $Pr=0.7$ ,  $Pe=1.0$ ,  $\beta=0.6$ ,  $Ha=0.1$ ,  $N_f=0.1$ ,  $D_f=0.05$ ,  $Ec=0.1$ .

The changes of  $Re_x^{1/2} C_f$ ,  $Re_x^{-1/2} Nu_x$ ,  $Re_x^{-1/2} Sh_x$ , and  $Re_x^{-1/2} Nn_x$  with variations of  $Ha$  are shown in Fig. 8 and Table 2 which indicates that higher  $Ha$  augments all of these quantities but they decrease for lowering  $S$  irrespective of  $We$ . The domain of the occurrence of dual solutions increases with  $Ha$ . It is noted that  $Ha^2 = \sigma B_0^2 / (b\rho)$  becomes large for higher magnetic strength and lower fluid density which accelerate the flow velocity. As a consequence, when stronger magnetic field is applied, it causes the velocity gradients at the surface and so the local skin friction coefficient is found to be higher.

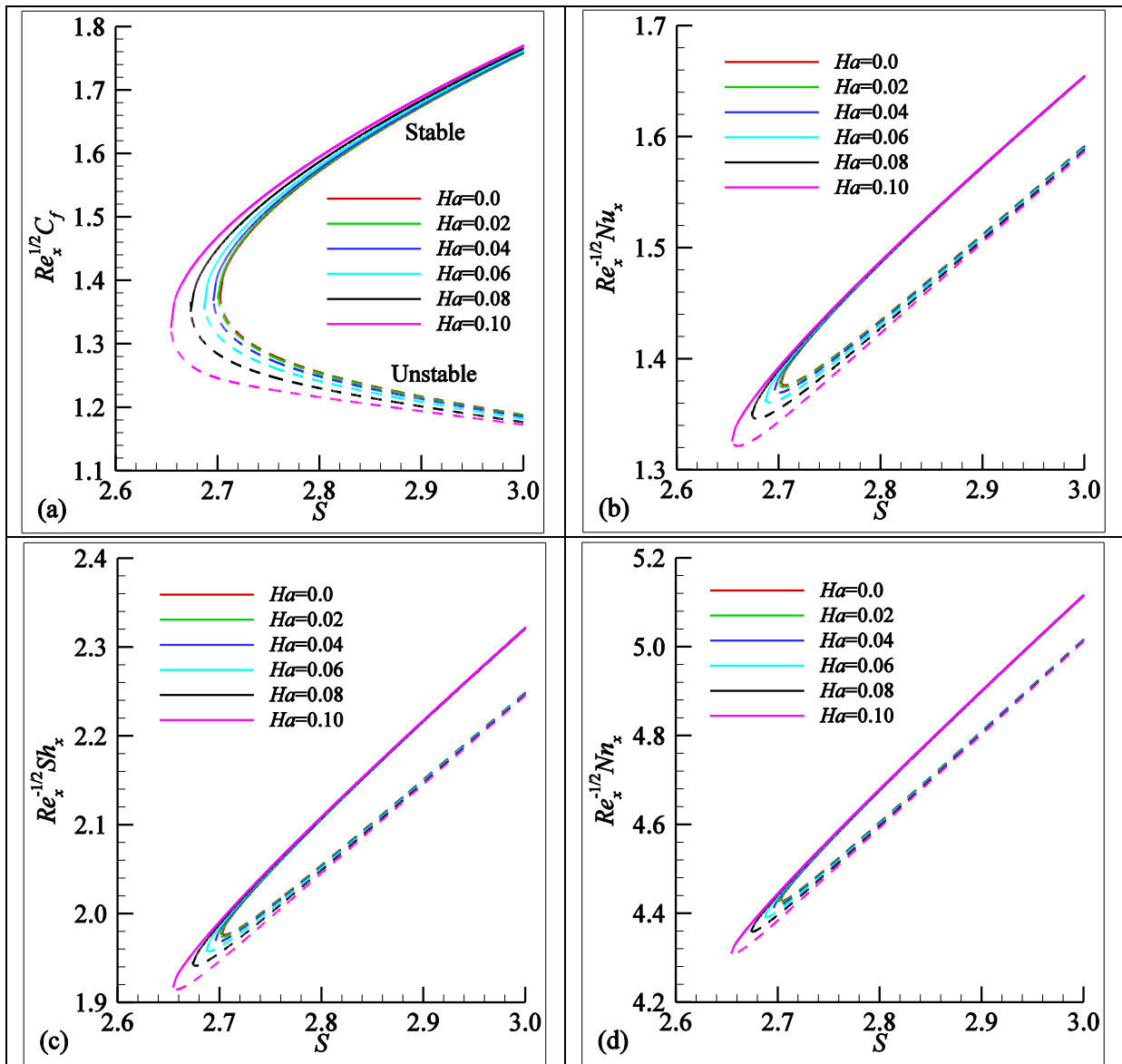


Fig. 8: Values of  $Re_x^{1/2} C_f$ ,  $Re_x^{-1/2} Nu_x$ ,  $Re_x^{-1/2} Sh_x$ , and  $Re_x^{-1/2} Nn_x$  when  $Pr=0.7$ ,  $Pe=1.0$ ,  $\beta=0.8$ ,  $N_t=0.1$ ,  $D_f=0.05$ ,  $Ec=0.1$ ,  $We=1.0$ .

Table 2: Variation of  $Re_x^{1/2} C_f$ ,  $Re_x^{-1/2} Nu_x$ ,  $Re_x^{-1/2} Sh_x$ , and  $Re_x^{-1/2} Nn_x$  when  $Pr=0.7$ ,  $Pe=1.0$ .

$\beta$	$Ha$	$N_t$	$D_f$	$Ec$	$We$	$S$	$Re_x^{1/2} C_f$	$Re_x^{-1/2} Nu_x$	$Re_x^{-1/2} Sh_x$	$Re_x^{-1/2} Nn_x$
0.5	0.10	0.1	0.05	0.10	1.0	3.5	2.16136	2.00313	2.78993	6.11067
0.6							2.17587	2.01507	2.80165	6.12740
0.7							2.13739	2.02403	2.80880	6.13781
0.8	0.0					2.8	1.57223	1.48588	2.10620	4.67591
	0.05						1.57819	1.48645	2.10693	4.67694
	0.10						1.59482	1.48798	2.10895	4.67977
		0.0				3.5	2.11357	1.98648	3.23283	6.55916
		0.2					2.20741	2.01983	2.34156	5.65640
		0.5					2.32940	2.07078	0.96198	4.25690
		0.1	0.0			2.8	1.57479	1.60315	2.08204	4.65143
			0.05				1.58762	1.52097	2.10096	4.67127
			0.08				1.59462	1.47102	2.11233	4.68316
			0.05	0.0		2.8	1.58011	1.55355	2.09299	4.66255

0.05			1.58762	1.52097	2.10096	4.67127
0.10			1.59482	1.48798	2.10895	4.67977
	0.0	3.4	1.36932	1.90841	2.64538	5.84447
	1.0		2.09528	1.94075	2.70372	5.92268
	2.0		1.81304	1.93612	2.69175	5.90579

## 5. Conclusion

In this study, the flow of MHD Casson or Carreau fluids with microorganisms over a permeable shrinking surface is considered. By solving the dimensionless governing equations by shooting method, we investigate the effects of non-Newtonian Casson parameter, Eckert number, Dufour number, thermophoretic diffusivity parameter, Weissenberg number and Hartmann number on the local skin friction coefficient, local Nusselt number, local Sherwood number, and local density number of the microorganisms. Results are concluded as follows:

- (i) An increase in non-Newtonian Casson parameter, Dufour number, thermophoretic diffusivity parameter and Hartmann number causes a significant increase in local skin friction coefficient, local Nusselt number, local Sherwood number, and local density number of the microorganisms.
- (ii) Higher Weissenberg number diminishes all of the above quantities.
- (iii) However, local skin friction coefficient, local Nusselt number, local Sherwood number, and local density number of the microorganisms are substantially decreased by increasing suction parameter whatever the values of other parameters.
- (iv) Dual solutions are observed over a wider region for higher values of non-Newtonian Casson parameter, Dufour number, thermophoretic diffusivity parameter, Eckert number and Hartmann number. On the contrary, the existence of dual solutions shrinks by larger Weissenberg number.

The present study can be extended for unsteady flow and stagnation point flow over a stretching/shrinking sheet.

## References

- Akbar, N.S., Nadeem, S., Haq, R.U., & Ye, S. (2014): MHD stagnation point flow of Carreau fluid toward a permeable shrinking sheet: Dual solutions. *Ain Shams Engineering Journal*, Vol. 5, No. 4, pp. 1233-1239. <https://doi.org/10.1016/j.asej.2014.05.006>
- Asogwa, K.K. & Ibe, A.A. (2020): A study of MHD Casson fluid flow over a permeable stretching sheet with heat and mass transfer. *Journal of Engineering Research and Reports*, Vol. 16, No. 2, pp. 10-25.
- Atif, S.M., Hussain, S., & Sagheer, M. (2019): Magnetohydrodynamic stratified bio-convective flow of micropolar nanofluid due to gyrotactic microorganisms. *AIP Advances*, Vol. 9, No. 2, pp. 25208-025208-16. <https://doi.org/10.1063/1.5085742>
- Bhattacharyya, K. (2011): Dual solutions in boundary layer stagnation-point flow and mass transfer with chemical reaction past a stretching/shrinking sheet. *International Communications in Heat and Mass Transfer*, Vol. 38, No. 7, pp. 917-922. <https://doi.org/10.1016/j.icheatmasstransfer.2011.04.020>
- Biswas, N., Datta, A., Manna, N.K., Mandal, D.K., & Gorla, R.S.R. (2021): Thermo-bio-convection of oxytactic microorganisms in porous media in the presence of magnetic field. *International Journal of Numerical Methods for Heat & Fluid Flow*, Vol. 31, No. 5, pp. 1638-1661. <https://doi.org/10.1108/HFF-07-2020-0410>
- El-Aziz, M.A. (2016): Dual solutions in hydromagnetic stagnation point flow and heat transfer towards a stretching/shrinking sheet with non-uniform heat source/sink and variable surface heat flux. *Journal of the Egyptian Mathematical Society*, Vol. 24, No. 3, pp. 479-486. <https://doi.org/10.1016/j.joems.2015.09.004>
- Freidoonimehr, N. & Rahimi, A.B. (2017): Exact-solution of entropy generation for MHD nanofluid flow induced by a stretching/shrinking sheet with transpiration: Dual solution, *Advanced Powder Technology*, Vol. 28, No. 2, pp. 671-685. <https://doi.org/10.1016/j.apt.2016.12.005>
- Ghosh, S., Mukhopadhyay, S., & Vajravelu, K. (2016): Dual solutions of slip flow past a nonlinearly shrinking permeable sheet, *Alexandria Engineering Journal*, Vol. 55, No. 2, pp. 1835-1840. <https://doi.org/10.1016/j.aej.2016.04.002>
- Hamid, M., Usman, M., Khan, Z.H., Ahmad, R., & Wang, W. (2019): Dual solutions and stability analysis of flow and heat transfer of Casson fluid over a stretching sheet. *Physics Letters A*, Vol. 383, pp. 2400-2408. <https://doi.org/10.1016/j.physleta.2019.04.050>
- Haq, R.U., Sajjad, T., Ullah, M.Z., Alshomrani, A.S., & Tlili, I. (2020): Dual nature solutions of water-based carbon nanotubes along a shrinking surface in the presence of thermal radiation and viscous dissipation.

- International Communications in Heat and Mass Transfer, Vol. 119, pp. 1-11. <https://doi.org/10.1016/j.icheatmasstransfer.2020.104938>
- Hayat, T., Shehzad, S.A., & Alsaedi, A. (2012): Soret and Dufour effects on magnetohydrodynamic (MHD) flow of Casson fluid. Applied Mathematics and Mechanics, Vol. 33, No. 10, pp. 1301–1312. <https://doi.org/10.1007/s10483-012-1623-6>
- Ishak, A., R. Nazar, R., Arifin, N.M., & Pop, I. (2008): Dual solutions in mixed convection flow near a stagnation point on a vertical porous plate. International Journal of Thermal Sciences, Vol. 47, No. 4, pp. 417-422. <https://doi.org/10.1016/j.ijthermalsci.2007.03.005>
- Ishak, A., Nazar, R., & Pop, I. (2009): Dual solutions in mixed convection boundary layer flow of micropolar fluids. Communications in Nonlinear Science and Numerical Simulation, Vol. 14, No. 4, pp. 1324-1333. <https://doi.org/10.1016/j.cnsns.2008.01.017>
- Khan, M., Hashim, Hafeez, A. (2017): A review on slip-flow and heat transfer performance of nanofluids from a permeable shrinking surface with thermal radiation: Dual solutions. Chemical Engineering Science, Vol. 173, pp. 1-11. <https://doi.org/10.1016/j.ces.2017.07.024>
- Khashiie, N.S., Arifin, N.M., Pop, I., & Nazar, R. (2021): Dual solutions of bioconvection hybrid nanofluid flow due to gyrotactic microorganisms towards a vertical plate. Chinese Journal of Physics, Vol. 72, pp. 461–474. <https://doi.org/10.1016/j.cjph.2021.05.011>
- Lund, L.A., Omar, Z., Khan, I. (2019): Analysis of dual solution for MHD flow of Williamson fluid with slippage. Heliyon, 5 (2019) e01345, 1-20. Lund, L. A., Omar, Z., & Khan, I. (2019). Analysis of dual solution for MHD flow of Williamson fluid with slippage. Heliyon, Vol. 5, No. 3, pp. e01345–e01345. <https://doi.org/10.1016/j.heliyon.2019.e01345>
- Mahanthesh, B., Animasaun, I.L., Rahimi-Gorji, M., & Alarifi, I.M. (2019): Quadratic convective transport of dusty Casson and dusty Carreau fluids past a stretched surface with nonlinear thermal radiation, convective condition, and non-uniform heat source/sink. Physica A, Vol. 535, pp. 1-16. <https://doi.org/10.1016/j.physa.2019.122471>
- Mondal, S.K. & Pal, D. (2020): Computational analysis of bio-convective flow of nanofluid containing gyrotactic microorganisms over a nonlinear stretching sheet with variable viscosity using HAM. Journal of Computational Design and Engineering, Vol. 7, No. 2, pp. 251–267.
- Mousavi, S.M., Rostami, M.N., Yousefi, M., Dinarvand, S., Pop, I., & Sheremet, M.A. (2021): Dual solutions for Casson hybrid nanofluid flow due to a stretching/shrinking sheet: A new combination of theoretical and experimental models. Chinese Journal of Physics, Vol. 71, pp. 574–588. <https://doi.org/10.1016/j.cjph.2021.04.004>
- Nagendra, N., Venkateswarlu, B., Boulahia, Z., Amanulla, C.H., & Ramesh, G.K. (2022): Magneto Casson-Carreau fluid flow through a circular porous cylinder with partial slip. Journal of Applied and Computational Mechanics, Vol. 8, No. 4, pp. 1208–1221. <https://doi.org/10.22055/jacm.2021.38390.3215>
- Qasim, M. & Noreen, S. (2014): Heat transfer in the boundary layer flow of a Casson fluid over a permeable shrinking sheet with viscous dissipation. The European Physical Journal Plus, Vol. 129, No. 7, pp. 1-8. <https://doi.org/10.1140/epjp/i2014-14007-5>
- Raju, C.S.K. & Sandeep, N. (2016): Unsteady three-dimensional flow of Casson–Carreau fluids past a stretching surface. Alexandria Engineering Journal, Vol. 55, No. 2, pp. 1115–1126. <https://doi.org/10.1016/j.aej.2016.03.023>
- Roy, N.C. (2020): Mathematical approach of demarcation of dual solutions for a flow over a shrinking surface. Chinese Journal of Physics, Vol. 68, pp. 514–532. <https://doi.org/10.1016/j.cjph.2020.10.003>
- Roy, N.C. & Saha, G. (2022): Heat and Mass Transfer of Dusty Casson Fluid over a Stretching Sheet. Arabian Journal for Science and Engineering, Vol. 47, No. 12, pp. 16091–16101. 16091–16101. <https://doi.org/10.1007/s13369-022-06854-x>
- Sandeep, N. & Sulochana, C. (2015): Dual solutions for unsteady mixed convection flow of MHD micropolar fluid over a stretching/shrinking sheet with non-uniform heat source/sink, Engineering Science and Technology, an International Journal, Vol. 18, No. 4, pp. 738-745. <https://doi.org/10.1016/j.jestch.2015.05.006>
- Saravana, R., Sailaja, M., Reddy, R.H. (2019): Effect of aligned magnetic field on Casson fluid flow over a stretched surface of non-uniform thickness. Nonlinear Engineering, Vol. 8, pp. 283–292. <https://doi.org/10.1515/nleng-2017-0173>
- Singh, G. & Chamkha, A.J. (2013): Dual solutions for second-order slip flow and heat transfer on a vertical permeable shrinking sheet. Ain Shams Engineering Journal, Vol. 4, No. 4, pp. 911-917. <https://doi.org/10.1016/j.asej.2013.02.006>
- Subhashini, S.V., Samuel, N., & Pop, I. (2012): Numerical investigation of dual solutions for double-diffusive convection from a permeable horizontal flat plate. International Journal of Heat and Mass Transfer, Vol. 55, No. 19–20, pp. 4981-4986. <https://doi.org/10.1016/j.ijheatmasstransfer.2012.04.036>

- Subhashini, S.V., Sumathi, R., & Pop, I. (2013): Dual solutions in a thermal diffusive flow over a stretching sheet with variable thickness, *International Communications in Heat and Mass Transfer*, Vol. 48, pp. 61-66. <https://doi.org/10.1016/j.icheatmasstransfer.2013.09.007>
- Subhashini, S.V. & Sumathi, R. (2014): Dual solutions of a mixed convection flow of nanofluids over a moving vertical plate. *International Journal of Heat and Mass Transfer*, Vol. 71, pp. 117-124. <https://doi.org/10.1016/j.ijheatmasstransfer.2013.12.034>
- Turkyilmazoglu, M. (2012): Dual and triple solutions for MHD slip flow of non-Newtonian fluid over a shrinking surface. *Computers Fluids*, Vol. 70, pp. 53-58. <https://doi.org/10.1016/j.compfluid.2012.01.009>
- Ullah, I., Alkanhal, T.A., Shafie, S., Nisar, K.S., Khan, I., & Makinde, O.D. (2019): MHD slip flow of Casson fluid along a nonlinear permeable stretching cylinder saturated in a porous medium with chemical reaction, viscous dissipation, and heat generation/absorption. *Symmetry*, Vol. 11, No. 4, pp. 531. <https://doi.org/10.3390/sym11040531>
- Waqas, H., Naseem, R., Muhammad, T., & Farooq, U. (2021): Bioconvection flow of Casson nanofluid by rotating disk with motile microorganisms. *Journal of Materials Research and Technology*, Vol. 13, pp. 2392-2407. <https://doi.org/10.1016/j.jmrt.2021.05.092>
- Xu, H. & Liao, S-J. (2008): Dual solutions of boundary layer flow over an upstream moving plate. *Communications in Nonlinear Science and Numerical Simulation*, Vol. 13, No. 2, pp. 350-358. <https://doi.org/10.1016/j.cnsns.2006.04.008>
- Yusuf, T.A., Mabood, F., Prasannakumara, B.C., & Sarris, I.E. (2021): Magneto-Bio-convection Flow of Williamson Nanofluid over an Inclined Plate with Gyrotactic Microorganisms and Entropy Generation. *Fluids*, Vol. 6, No. 3, pp. 109. <https://doi.org/10.3390/fluids6030109>
- Zheng, L., Niu, J., Zhang, X., & Ma, L. (2012): Dual solutions for flow and radiative heat transfer of a micropolar fluid over stretching/shrinking sheet. *International Journal of Heat and Mass Transfer*, Vol. 55, No. 25–26, pp. 7577-7586. <https://doi.org/10.1016/j.ijheatmasstransfer.2012.07.067>